Journal of The Electrochemical Society, **163** (5) H286-H291 (2016)
0013-4651/2016/163(5)/H286/6/$33.00 © The Electrochemical Society

An Imaging Ellipsometry Approach to Dissolved Oxygen Measurement on Surface Tethered Weak Polyelectrolyte Modified Electrode

Wei Liu,[a,b] Meng Li,[a,b] Bei'er Lv,[c] YanYan Chen,[d] Hongwei Ma,[d] Ana S. Viana,[e] Jorge P. Correia,[e] and Gang Jin[a,z]

[a]*NML, Institude of Mechanics, Chinese Academy of Sciences, Beijing 100190, People's Republic of China*
[b]*University of Chinese Academy of Sciences, Beijing 100049, People's Republic of China*
[c]*Physical Chemistry I, Department of Chemistry and Biology, Siegen University, 57076 Siegen, Germany*
[d]*Suzhou Institute of Nano-Tech and Nano-Bionics, Chinese Academy of Science, Suzhou 21513, People's Republic of China*
[e]*Centro de Química e Bioquímica, Departamento de Química e Bioquímica, Faculdade de Ciíncias da Universidade de Lisboa, Ed. C8, Campo Grande, 1749-016 Lisboa, Portugal*

Electro - total internal reflection ellipsometry has been reported as a phase sensitive ellipsometry technique to observe the redox reactions on the surface of the electrode. In this work, with the imaging ellipsometry, we have used Electro-total internal reflection imaging ellipsometry (Electro-TIRIE) to measure the dissolved oxygen concentration on the surface tethered weak polyelectrolyte brush, carboxylated poly(oligo(ethylene glycol) methacrylate-random-2-hydroxyethylmethacrylate), modified electrode. The cyclic voltammetry has shown despite the covering of the weak polyelectrolyte brush, the electrode could still reduce the dissolved oxygen and Electro-TIRIE technique could unveil the different swelling behavior of the brushes during the reduction. The difference may be attributed to the electro-active probe permeability of the brushes. With the imaging ellipsometry, we proposed a parallel dissolved oxygen measurement. Compared with our previous results, the optical signal noise ratio has been enhanced 10 times and the measurement time has reduced from 30 minutes to 10 minutes.

Manuscript submitted October 7, 2015; revised manuscript received January 11, 2016. Published January 27, 2016.

Total internal reflection ellipsometry (TIRE) technique has been proposed as a powerful tool to study the redox reactions on the surface of the electrode for its high interface sensitivity in the ellipsometry phase shift, Δ.[1] The high interface sensitivity of TIRE arises from its using evanescent wave as the detection probe.[2,3] By combining the imaging techonology, total internal reflection imaging ellipsometry (TIRIE) has been developed.[4] Besides the high interface sensitivity, the imaging ellipsometry approach makes TIRIE useful for multi-sample detection for various bioprocesses.[5,6] For example, we take TIRIE as the biosensor to detect cluster of differentiation 146 (CD146), a cell adhesion molecule used as a marker for endothelial cell lineage, quantitatively.[7] By introducing low noise imaging device[8] and optimizing the incident angle, the polarization of the light beam and the thickness of the introduced thin gold layer,[9] we use TIRIE biosensor to investigate the behavior of giant lipid vesicles (GUVs) interacting with an adhesive surface coated with poly-l-lysine.[10]

The dissolved oxygen measurement is of great importance in various areas, such as physical, chemical and environmental applications.[11–16] Our previous work has demonstrated that Electro-TIRE can be used to monitor the dissolved oxygen concentration on Clark electrode.[1] However, the optical signal noise ratio (OSNR) is barely about 30, which is insufficient for the dissolved oxygen sensing for practical applications. A second problem is that it is time-consuming to determine the dissolved oxygen concentration of a sample: at least 30 minutes. However, applications require relatively fast oxygen concentration measurement.[17–19] In this paper, to increase OSNR, a surface tethered weak polyelectrolyte brush (STWPB), carboxylated poly(oligo(ethylene glycol) methacrylate-random-2-hydroxyethylmethacrylate) (poly(OEGMA-r-HEMA)), has been introduced on the TIRIE sensing chip. Poly(OEGMA-r-HEMA) is reported sensitive to local pH change in the aqueous medium. With the imaging ellipsometry, a parallel dissolved oxygen measurement has been proposed to reduce the measurement time.

Experimental

Principle and STWPB preparation.—When we apply a polarized potential to the electrode, the dissolved oxygen is reduced on the electrode surface as follows:[20]

$$\text{Cathodic reaction:} \quad O_2 + 2H_2O + 4e^- \rightarrow 4OH^-$$

Because of the hydroxyl ions generated by the reduction of the dissolved oxygen, local pH of the electrolyte increases in the neighborhood of the cathode electrode.

Governed by the electrostatic interactions and the osmotic pressure,[21,22] carboxylated poly(OEGMA-r-HEMA) is reported sensitive to pH and ionic strength of the medium.[23] Under a given $[Na^+]$(<15 mM), its swelling behavior mainly depends on pH of the electrolyte, varying from pH 2 to 7.4:[24] with the increase of pH, COOH groups in the structure dissociate as COO^- groups. Thus, the polyelectrolyte brush stretches because of the electrostatic interactions among COO^- groups. On the other hand, local pH of the electrolyte in the neighborhood of the electrode would be modulated owing to the hydroxyl ions generated by the dissolved oxygen reduction. As is reported in Ref. 25, the process is determined by the diffusion of hydroxyl ions in the structure of the weak polyelectrolyte. In general, the principle is shown as Fig. 1.

Three different thickness brushes were prepared as previously described:[24,26] 4 nm, 8 nm and 16 nm. Briefly, TIRIE chips (SF10 glass slides covered with a 2-nm-thick Cr adhesive under-layer and a 50-nm-thick gold film) were first modified with initiator thiol and diluent thiol via a self-assembled monolayer (SAM) technique. After the modification, surface initiated polymerization (SIP) was initiated by immersing the SAM modified chips to a reaction solution. By controlling the SIP time, the polymer thickness varied. Finally, the polyelectrolyte surfaces were generate by substituting carboxyl groups for hydroxyl groups of poly(OEGMA-r-HEMA).

Chemicals.—PBS buffer (pH 7.4) is purchased from Sigma-Aldrich, hydrochloric acid (HCl) of 37% concentration from Beijing Chemical Works. All the compounds used in this work are in analytical grade without further purification. Ultrapure water is obtained from a MILLI-Q purification system (18.2 MΩ at room temperature) and used to prepare all the solutions.

To detect swelling behavior of carboxylated poly(OEGMA-r-HEMA) from the dissolved oxygen reduction, the diluted PBS with $[Na^+] = 1.5$ mM is used as the electrolyte, pH of which is adjusted to

[z]E-mail: gajin@imech.ac.cn

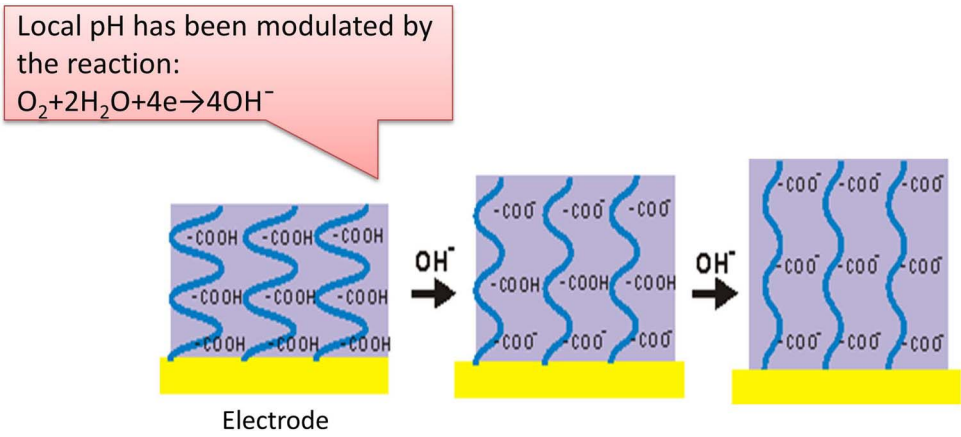

Figure 1. Local pH modulation by the dissolved oxygen reduction would stretch carboxylated poly(OEGMA-r-HEMA).The modulation is determined by the diffusion of OH^- in the structure.

the desired range with HCl. Different dissolved oxygen concentration samples are obtained by bubbling mixed oxygen and nitrogen.

Instrumentation.—SENTECH SE400 multiple angle laser ellipsometer has been used to verify the dry thickness of carboxylated poly(OEGMA-r-HEMA) modified TIRIE chip. The wavelength of the light beam is 632.8 nm and the angle of incidence is fixed at 70°.

Figure 2a illustrates the system setup, Electro-TIRIE, used for all experiments described in this paper. The electrochemical experiments are performed using a VersaSTAT 3 electrochemical system (Princeton, U.S.A). A SF10 trapezoidal prism is used with a Xe lamp as the light source and a high-speed CCD camera as the detector. After passing through an aperture, the 632.8 nm light beam is expanded by a collimating system. By passing a polarizer and a compensator, the polarized collimated beam is obtained, which propagates perpendicularly to the prism and onto the sensing surface. When the incident angle is optimized as 57°, larger than the critical angle, the evanescent wave appears sharply at the sensing surface to detect the interaction in very shallow depth from the surface (around 100 nm). The reflected light carrying the surface information is then imaged by a CCD camera after passing an analyzer. The system works under the null and off-null mode, which almost fulfills the null condition on the sensing surface when no redox reactions occur and detects the optical thickness change of carboxylated poly(OEGMA-r-HEMA) under the off-null condition when the dissolved oxygen is reduced. Combined with an external electrochemical working station, this configuration allows for simultaneously TIRIE detection of the optical variation on the sensing surfaces of both detection units and the electrochemical measurement. During the measurement, the optical variation of the sensing surface caused by the dissolved oxygen reduction is recorded by TIRIE in grayscale as in Fig. 3b.

Since the imaging ellipsometry enjoys high throughput, as shown in Figs. 2b and 3a, a parallel detection cell is designed. The cell has two independent detection units. For each unit, a Ag/AgCl electrode serves as the reference and a Ag electrode as the counter. A 50 nm Au/Cr/SF10 glass slide with the brush is the sensing surfaces and cathodes of both units. During the parallel detection for the dissolved oxygen measurement, one unit works as the reference cell. A sample with the given dissolved oxygen concentration is measured in this unit, while the sample with unknown concentration is measured in the other unit. By comparing the signals of the both units, the dissolved concentration of a sample can be determined in a relatively short time.

Results and Discussion

Dissolved oxygen reduction on the STWPB modified electrode.—Before all the electrochemical experiments, the dry thicknesses of carboxylated poly(OEGMA-r-HEMA) have been calculated from the ellipsometric parameters of the chip in Table I. For many organic films, the refractive index is around $1.3 \sim 1.6$.[27] In our situation, we set it as 1.4 which is suitable for most organic monolayers. Then, we have measured the maximum TIRIE signal change caused by the brush swelling. Two electrolytes have been used with pH 1 when carboxylated poly(OEGMA-r-HEMA) remains unstretched and pH 7.4 during which the polyelectrolyte reaches its maximum length.[24]

With the increase of the brush thickness, carboxylated poly(OEGMA-r-HEMA) stretches owing to more dissociation of COOH groups in the structure. Thus, as is demonstrated in Fig. 4, the maximum TIRIE signal increases: 6 ± 0.68 grayscale for 4 nm polyelectrolyte, 22 ± 1.23 grayscale for 8 nm and 36 ± 1.88 grayscale for 16 nm, which gives the largest optical signal change.

On the other hand, STWPB covered on the electrode could block the transfer of the electrons, which would make the dissolved oxygen reduction less efficiency.[28] To estimate the efficiency of the dissolved reduction on the weak polyelectrolyte modified electrode, cyclic voltammetry (CV) has been performed to study the swelling behavior of carboxylated poly(OEGMA-r-HEMA). The dissolved oxygen saturated electrolyte is used with pH 1 and the scan rate is 50 mV/s. The distance between the sensing surface and the dissolved oxygen permeable membrane is adjusted to 8 mm.

The reduction of the dissolved oxygen is a diffusion-limited reaction. The hydroxyl ion diffusion coefficient is $D = 5.273 \times 10^{-9}$ m^2/s.[29] The diffusion distance for 1 second can be estimated by $(2Dt)^{1/2} \approx 10^{-4}$ m. Under the semi-infinite boundary condition, the hydroxyl ion concentration change can be estimated by[30]

$$C_{OH} = -D^{-1/2}(NF\pi^{1/2})^{-1}\int_0^t j(\tau)(t-\tau)^{-1/2}d\tau \qquad [1]$$

where j is the current density obtained by CV, N is the number of electrons transfered during the oxygen reduction and F is the Farady constant. Fig. 5c is the calculated hydroxyl ion concentrations vs. potential based on Eq. 1. As is expected, the thicker STWPB generates less OH^-, because the polyelectrolyte blocks the diffusion of the dissolved oxygen.

The optical signals of the three STWPBes have been recorded synchronously in Fig. 5b. In fact, besides the swelling behavior of the weak polyelectrolyte brushes, another two factors from the potential modulation of the electrode will also contribute to the optical signals: the complex refractive index change of the gold and the electric double layer variation.[30] The influences of the both factors will be discussed in detail later.

During the sweep from 0 V to −0.6 V, the significant optical increases for all the brushes start at −0.52 V for 16 nm, −0.44 V for 8 nm and −0.38 V for 4 nm (denoted as A, B and C in Fig. 5b). Compared with Fig. 5c, at these potentials, the generated hydroxyl ions for all the brushes are the same, around 11 μmol/L. It indicates

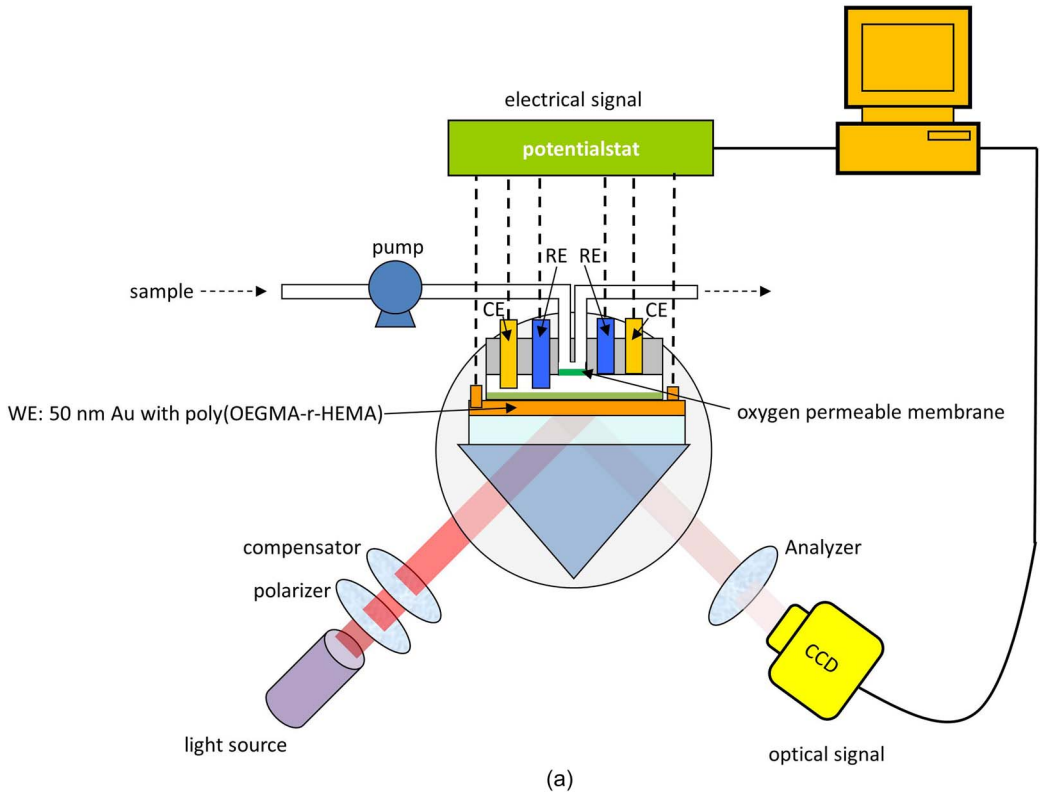

(a)

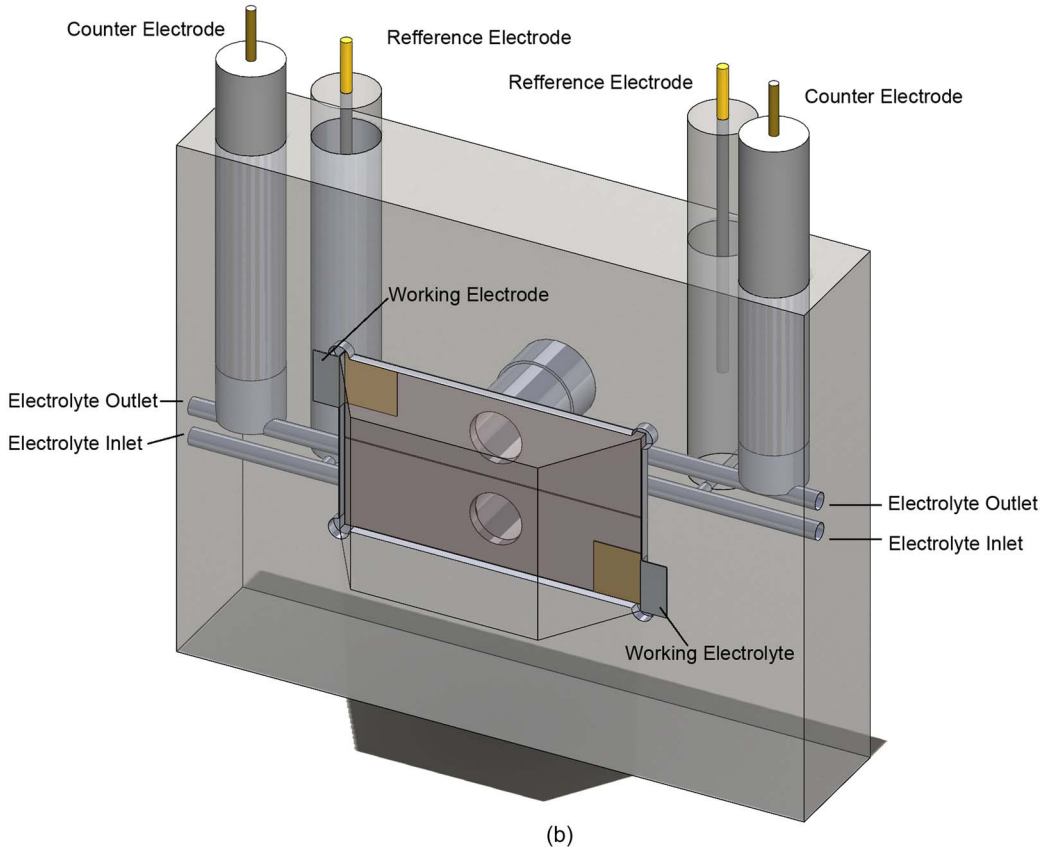

(b)

Figure 2. (a) Schematic illustration of Electro-TIRIE system and (b) the parallel detection cell. The cell has two independent detection units. Each unit consists two compartments separated by the oxygen permeable membrane: one for the electrolyte, the other for the sample solution. In the electrolyte compartment, the weak polyelectrolyte modified gold film works as the sensing surface for TIRIE and the working electrode of the reaction cell. In the sample compartment, the sample with different oxygen concentrations is delivered into the cell.

Table I. Ellipsometric parameters and calculated brush thickness on STWPB modified TIRIE chip.

	ψ /°	Δ /°	Thickness ($n = 1.4$)/nm
TIRIE chip	42.779 ± 0.008	109.713 ± 0.158	
4 nm STWPB	42.132 ± 0.011	105.703 ± 0.320	3.901 ± 0.104
8 nm STWPB	41.841 ± 0.027	102.079 ± 0.384	7.948 ± 0.086
16 nm STWPB	39.841 ± 0.081	94.583 ± 0.572	15.210 ± 0.128

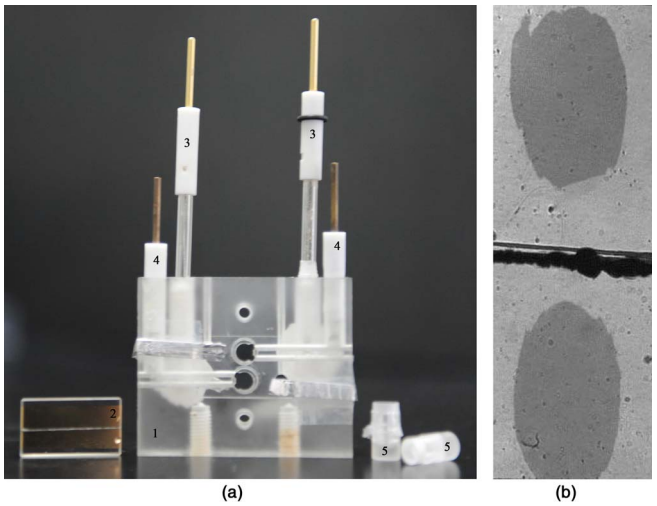

Figure 3. (a)The photo of the parallel detection cell. 1: the cell, 2: TIRIE chip with two independent reaction areas, 3: Ag/AgCl reference electrodes, 4: Ag counter electrodes, 5: sample compartments with the oxygen permeable membranes; (b) Detection image in grayscale. Both units have been recorded.

a pH threshold for the electrolyte, which is consistent with, Ref. 24 above which, the polyelectrolyte films begin to swell. However, when the potential decreases from −0.55 V to −0.6 V, the optical signals of 4 nm and 8 nm brushes drop a little while that of the 16 nm one is constantly increasing. This might be because under the circumstances, the complex refractive index change of the gold and the electric double layer variation of the electrolyte play an important role in the optical signal when the polyelectrolyte brushes are stretched to a certain extent. Actually, these two factors decrease the optical signal change caused by the brush swelling. For example, compared with the maximum TIRIE signal change, 6 grayscales, in Fig. 4 when no potential is applied to the surface, the maximum optical signal change for 4 nm brush is only 4 grayscales during the sweep.

On the other hand, when the potential sweeps from −0.6 V to 0 V, although all the brushes have returned to their initial thicknesses in the end, the optical signals suggest the transformations of the brushes do not to follow their original swelling paths and the thicknesses of the brushes influence the "shrinking" process. For example, at the potential of −0.48 V, the 4 nm brush during the "shrinking" process is thiner than itself during the "swelling" process while the 16 nm brush is thicker and the 8 nm brush is the same at the potential for

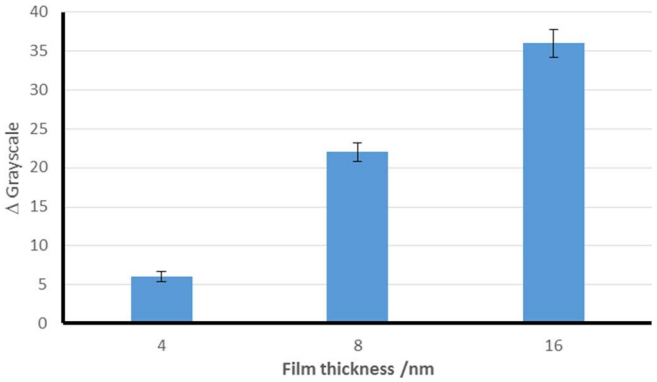

Figure 4. The thickness of carboxylated poly(OEGMA-r-HEMA) vs. the maximum TIRIE signal change caused by pH modulation.

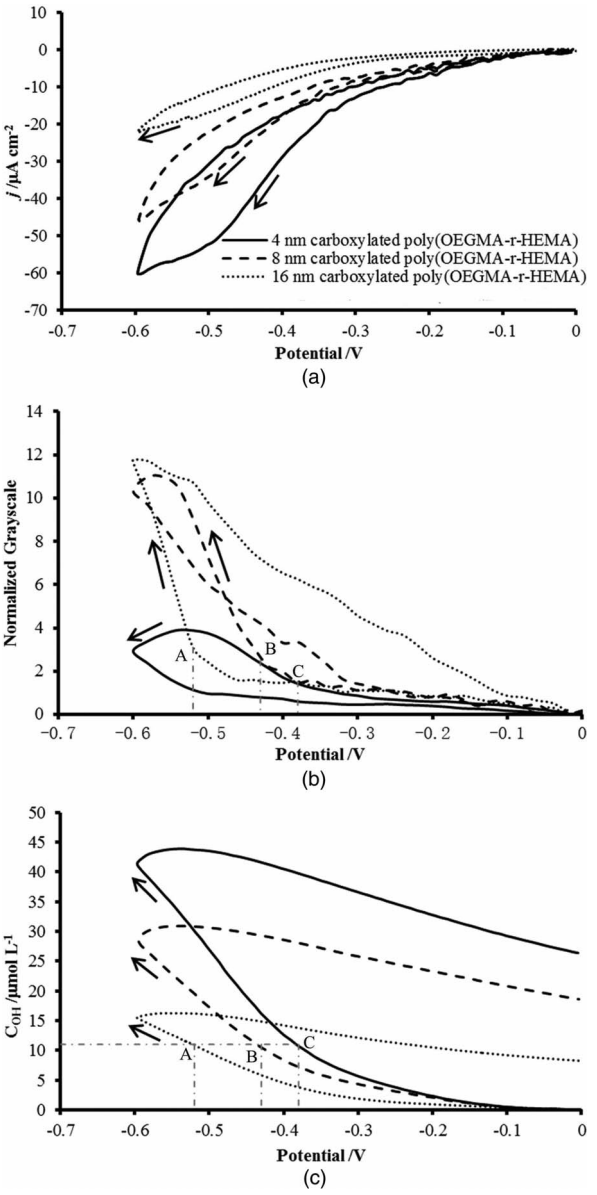

Figure 5. (a) CV diagram for carboxylated poly(OEGMA-r-HEMA) of different thicknesses. (b) Synchronous optical signal vs. potential. (c) The calculated hydroxyl ion concentration based on the current density. The arrows indicate the scan direction.

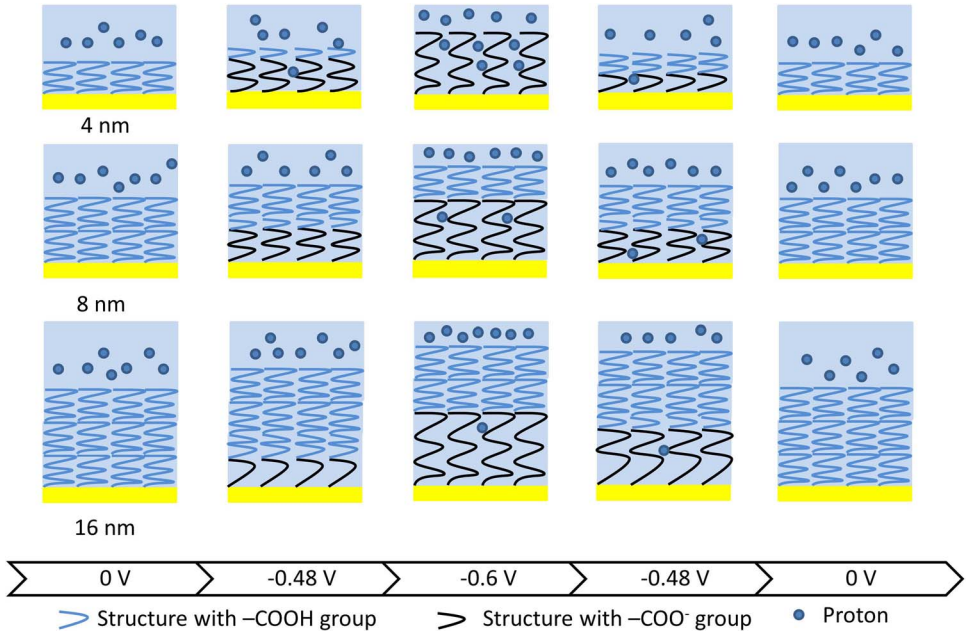

Figure 6. The swelling behavior of carboxylated poly(OEGMA-r-HEMA) with different thicknesses under CV sweep from 0 V to −0.6 V. The dissociation of COOH groups starts from the bottom of the brush is because the dissolved oxygen should be reduced at the electrode surface rather than the top of the brush. Thus, the hydroxyl ion concentration will decrease from the gold surface into the aqueous phase gradually, which makes the bottom of the brush tend to stretch.

both processes. In fact, for the 8 nm brush, the "shrinking" process can be divided into two stages: from −0.6 V to −0.48 V, the brush is thiner than itself during the "swelling" process and from −0.48 V to 0 V, the brush is thicker. The phenomenon might be attributed to the permeability of protons in the structure. As is pointed out by Ref. 28, STWPB enjoys two states: swollen states allowing good electroactive probe permeability and the collapsed states, which hesitates the electron transfer. When STWPB stretches, the swollen states occupy the structure. The protons in the electrolyte are easy to diffuse into the structure. Otherwise, the collapsed states take up the STWPB. The diffusion is difficult. For a 4 nm polyelectrolyte, since the film is almost fully stretched, the structure is mainly COO^- groups, comparatively loose with COOH. Thus, the protons in the electrolyte easily diffuse into the brush, which causes the association of COOH are more favorable. For a 16 nm film, the top of the polyelectrolyte are occupied by the collapsed COOH groups. It is difficult for the protons in the electrolyte to diffuse into the structure. Therefore, the association of COOH groups are gentle, which makes the brush "thicker" in shrinking process than itself in swelling process. For a 8 nm brush, the structure makes the permeability of the protons intermediate. The whole process of carboxylated poly(OEGMA-r-HEMA) with different thicknesses is illustrated as Fig. 6.

Dissolved oxygen measurement and parallel detection.—To detect the dissolved oxygen concentration in the sample, both 8 nm and 16 nm STWPB modified electrodes have been used to measure the dissolved oxygen saturated sample under −0.6 V vs. Ag/AgCl in Figs. 7a and 7b. During the measurement, the oxygen permeable membrane is adjusted to about 1 mm. As is discussed in our previous work,[1] for Clark electrode configuration, when the dissolved oxygen reduction reaches the steady state, the generated hydroxyl ion concentration is constant. It implies that the pH of the electrolyte at the sensing surface is also a steady state. Thus, the dissociation of the polyelectrolyte is stable.The synchronous variations of the current and the TIRIE signal indicate the carboxylated poly(OEGMA-r-HEMA) modified electrodes can be used to measure the dissolved oxygen. By comparing the signal variations of the both brushes (17 grayscale optical signal variation and 0.6 μA current change for 8 nm brush and 20 grayscale optical signal variation and 0.1 μA current change for 16 nm), 8 nm STWPB has been chosen for the measurement. Compared with our previous work on bare gold,[1] the optical signal is amplified by around 10 times while the current variation is decreased about 10 times. Since the noise of the given TIRIE system was around 0.05 grayscale, the OSNR was around 360, about 10 times larger than the previous result. Owing to the introduction of the reference unit, the measurement for one sample reduced from 30 minutes to 10 minutes.

By introducing 8 nm carboxylated poly(OEGMA-r-HEMA) on the electrode surface, as shown in Fig. 7c, not only the current change is proportional to the oxygen concentration in the sample ($y = 0.0807x + 0.0227$, $R^2 = 0.9937$), but the TIRIE signal variation ($y = 2.0442x + 0.0227$, $R^2 = 0.998$). The results have demonstrated that by introducing STWPB on the sensing surface and the imaging technology, the system can be used as a quick dissolved oxygen probe.

Since the dissolved oxygen measurement is fundamental for biochemical oxygen demand (BOD) measurement, we have reported using the STWPB modified electrode to monitor BOD in real sample.[31] Compared with the conventional BOD measurement method, the deviation of both optical and electrical signals are less than 10%.

Conclusions

Electro-TIRIE system has been used to observe the dissolved oxygen concentration on the carboxylated poly(OEGMA-r-HEMA) modified electrode. The CV has shown that the dissolved oxygen still could be reduced on 4 nm, 8 nm and 16 nm carboxylated poly(OEGMA-r-HEMA) modified TIRIE chip. Further, Electro-TIRIE technique unveils that in spite of the similar CV curves, the swelling behavior of the brushes of the different thicknesses could follow quite varied paths during the reduction process. The variation may lie in the difference of the electroactive probe permeability of the polyelectrolyte brush. With the imaging ellipsometry, we have used 8 nm carboxylated poly(OEGMA-r-HEMA) modified electrode to measure dissolved oxygen concentration. Compared with our previous results, the OSNR has been enhance 10 times and the measurement time has reduced from 30 minutes to 10 minutes.

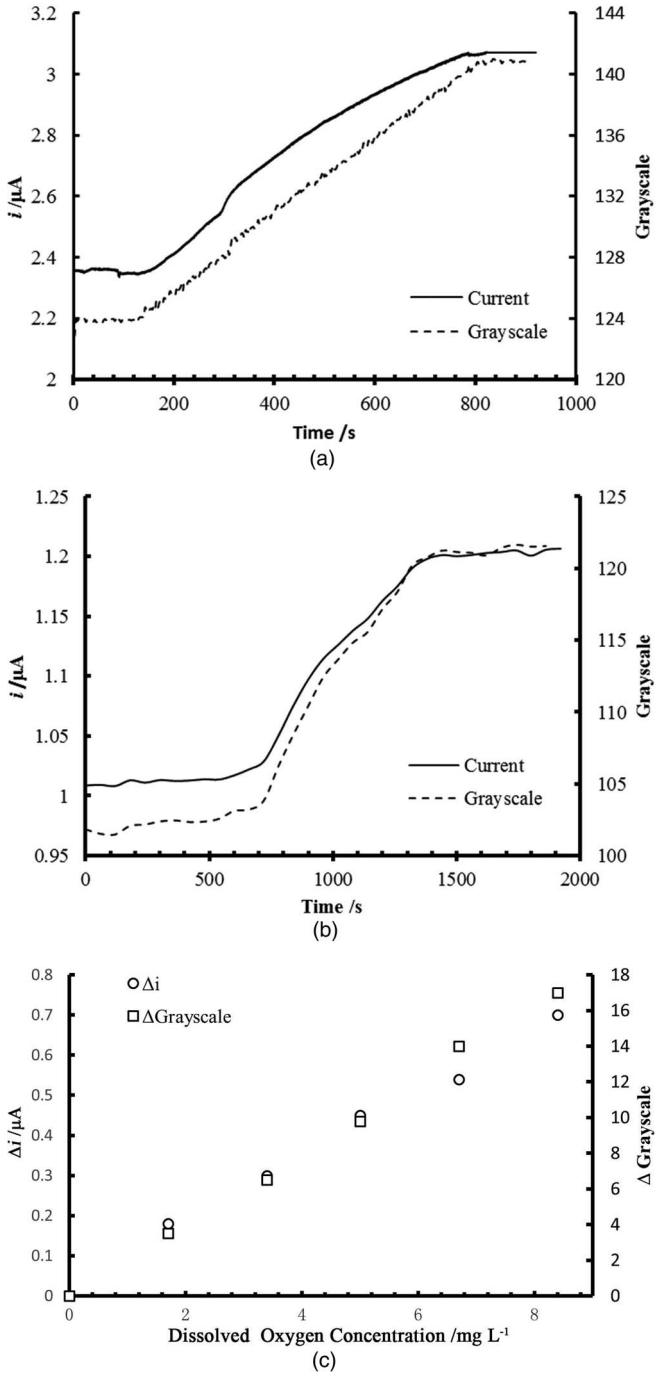

Figure 7. (a) The measurement of the saturated dissolved oxygen sample on 8 nm STWPB modified electrode. (b) The measurement of the saturated dissolved oxygen sample on 16 nm STWPB modified electrode. (c) The dissolved oxygen calibration curve.

Acknowledgments

The authors acknowledge the financial support to the National Natural Science Foundation of China (21305147, 11274345), to the International Science & Technology Cooperation Program of China (2015DFG32390), FCT project-UID/MULTI/00612/2013 to the National Basic Research Program of China (2009CB320302), to the National High Technology Research Development Program of China (2008AA02Z419), and to the Instrument Developing Project of the Chinese Academy of Sciences (KJCX2-YW-M04, KJCX2-YW-M03).

References

1. W. Liu, M. Li, and G. Jin, Using electrochemistry - total internal reflection ellipsometry technique to observe the dissolved oxygen reduction on clark electrode, *Electrochimica Acta*, **142**(0), 371 (2014).
2. M. Poksinski, H. Dzuho, J.-O. Järrhed, and H. Arwin, Total internal reflection ellipsometry, in: *Eurosensors XIV: The 14th European Conference on Solid-State Transducers: Book of Abstracts*, MIC, 2000, pp. 239–242.
3. H. Arwin, M. Poksinski, and K. Johansen, Total internal reflection ellipsometry: principles and applications, *Applied optics*, **43**(15), 3028 (2004).
4. Y. Chen, Z. Wang, Y. Meng, and G. Jin, Biosensor with total internal reflection imaging ellipsometry, *International Journal of Nanotechnology*, **4**(1), 171 (2007).
5. Y. Zhang, Y. Chen, and G. Jin, Serum tumor marker detection on pegylated lipid membrane using biosensor based on total internal reflection imaging ellipsometry, *Sensors and Actuators B: Chemical*, **159**(1), 121 (2011).
6. A. Gunnarsson, M. Bally, P. Jönsson, N. Médard, and F. Höök, Time-resolved surface-enhanced ellipsometric contrast imaging for label-free analysis of biomolecular recognition reactions on glycolipid domains, *Analytical chemistry*, **84**(15), 6538 (2012).
7. L. Liu, Y. Niu, Y. H. Meng, S. Chen, X. Y. Yan, and G. Jin, CD146 detection with real-time total internal reflection imaging ellipsometry, *Vol. 25 of IFMBE Proceedings*, Springer, New York, 2009, pp. 34–36.
8. L. Liu and G. Jin, Total internal reflection imaging ellipsometry (tirie) biosensor sensitivity improvement with low noise imaging device, in: *IS&T/SPIE Electronic Imaging*, International Society for Optics and Photonics, 2011, pp. 78750U–78750U.
9. L. Liu, Y. Niu, S. Chen, Y. Meng, H. Ma, and G. Jin, Optimization of evanescent wave imaging for the visualization of protein adsorption layers, *Science China Physics, Mechanics and Astronomy*, **53**(10), 1805 (2010).
10. L. Liu, A. Viallat, and G. Jin, Vesicle adhesion visualized with total internal reflection imaging ellipsometry biosensor, *Sensors and Actuators B: Chemical*, **190**, 221 (2014).
11. R. Gillanders, M. Tedford, P. Crilly, and R. Bailey, A composite thin film optical sensor for dissolved oxygen in contaminated aqueous environments, *Analytica chimica acta*, **545**(2), 189 (2005).
12. K. Tsukada, S. Sakai, K. Hase, and H. Minamitani, Development of catheter-type optical oxygen sensor and applications to bioinstrumentation, *Biosensors and bioelectronics*, **18**(12), 1439 (2003).
13. Y. Amao, T. Miyashita, and I. Okura, Optical oxygen sensing based on the luminescence change of metalloporphyrins immobilized in styrene–pentafluorostyrene copolymer film, *Analyst*, **125**(5), 871 (2000).
14. C. O. Moses, D. Kirk Nordstrom, J. S. Herman, and A. L. Mills, Aqueous pyrite oxidation by dissolved oxygen and by ferric iron, *Geochimica et Cosmochimica Acta*, **51**(6), 1561 (1987).
15. L. H. Gray, A. Conger, M. Ebert, S. Hornsey, and O. Scott, The concentration of oxygen dissolved in tissues at the time of irradiation as a factor in radiotherapy, *British Journal of Radiology*, **26**(312), 638 (1953).
16. K. Kaiho, Benthic foraminiferal dissolved-oxygen index and dissolved-oxygen levels in the modern ocean, *Geology*, **22**(8), 719 (1994).
17. B. Bandyopadhyay, A. Humphrey, and H. Taguchi, Dynamic measurement of the volumetric oxygen transfer coefficient in fermentation systems, *Biotechnology and Bioengineering*, **9**(4), 533 (1967).
18. A. A. Benedek and W. J. Heideger, Polarographic oxygen analyzer response: The effect of instrument lag in the non-steady state reaeration test, *Water Research*, **4**(9), 627 (1970).
19. I. J. Dunn and A. Einsele, Oxygen transfer coefficients by the dynamic method, *Journal of Applied chemistry and Biotechnology*, **25**(9), 707 (1975).
20. Y. H. Lee and G. T. Tsao, *Dissolved oxygen electrodes*, Springer, 1979.
21. N. Ayres, S. G. Boyes, and W. J. Brittain, Stimuli-responsive polyelectrolyte polymer brushes prepared via atom-transfer radical polymerization, *Langmuir*, **23**(1), 182 (2007).
22. J. Rühe, M. Ballauff, M. Biesalski, P. Dziezok, F. Gröhn, D. Johannsmann, N. Houbenov, N. Hugenberg, R. Konradi, S. Minko et al., Polyelectrolyte brushes, in: *Polyelectrolytes with Defined Molecular Architecture I*, Springer, 2004, pp. 79–150.
23. E. Zhulina, T. Birshtein, and O. Borisov, Theory of ionizable polymer brushes, *Macromolecules*, **28**(5), 1491 (1995).
24. Y. Zhang, B. Lv, Z. Lu, J. He, S. Zhang, H. Chen, and H. Ma, Predicting au–s bond breakage from the swelling behavior of surface tethered polyelectrolytes, *Soft Matter*, **7**(24), 11496 (2011).
25. S. E. Burke and C. J. Barrett, Acid-base equilibria of weak polyelectrolytes in multilayer thin films, *Langmuir*, **19**(8), 3297 (2003).
26. Y. Zhang, J. He, Y. Zhu, H. Chen, and H. Ma, Directly observed au–s bond breakage due to swelling of the anchored polyelectrolyte, *Chemical Communications*, **47**(4), 1190 (2011).
27. A. Ulman, An Introduction to Ultrathin Organic Films: From Langmuir–Blodgett to Self–Assembly, Academic press, 2013.
28. F. Zhou, H. Hu, B. Yu, V. L. Osborne, W. T. Huck, and W. Liu, Probing the responsive behavior of polyelectrolyte brushes using electrochemical impedance spectroscopy, *Anal Chem*, **79**(1), 176 (2007).
29. E. Samson, J. Marchand, and K. Snyder, Calculation of ionic diffusion coefficients on the basis of migration test results, *Materials and Structures*, **36**(3), 156 (2003).
30. S. Wang, X. Huang, X. Shan, K. J. Foley, and N. Tao, Electrochemical surface plasmon resonance: basic formalism and experimental validation, *Anal Chem*, **82**(3), 935 (2010).
31. W. Liu, M. Li, B. Lv, Y. Chen, H. Ma, and G. Jin, Using electrochemistry-total internal refection imaging ellipsometry to monitor biochemical oxygen demand on the surface tethered polyelectrolyte modified electrode, in: *SPIE BiOS*, International Society for Optics and Photonics, 2015, pp. 93360C–93360C.